SAGE-Hindawi Access to Research
International Journal of Electrochemistry
Volume 2011, Article ID 129182, 7 pages
doi:10.4061/2011/129182

Research Article

Investigation of the Performance of Au_{core}-Pd_{shell}/C as the Anode Catalyst of Direct Borohydride-Hydrogen Peroxide Fuel Cell

Hong Wang,[1] Ying Wang,[2] Xianyou Wang,[1] Peiying He,[1] Lanhua Yi,[1] Wei Yi,[1] and Xue Liu[1]

[1] *Key Laboratory of Environmentally Friendly Chemistry and Applications of Ministry of Education, School of Chemistry, Xiangtan University, Hunan 411105, China*
[2] *School of Chemical Engineering and Pharmacy, Wuhan Institute of Technology, Hubei 430073, China*

Correspondence should be addressed to Xianyou Wang, wxianyou@yahoo.com

Received 26 April 2011; Accepted 7 September 2011

Academic Editor: Carlos F. Zinola

The carbon-supported bimetallic Au-Pd catalyst with core-shell structure is prepared by successive reduction method. The core-shell structure, surface morphology, and electrochemical performances of the catalysts are characterized by X-ray diffraction (XRD), transmission electron microscopy (TEM), ultraviolet-visible absorption spectrometry, linear sweep voltammetry, and chronopotentiometry. The results show that the Au-Pd/C catalyst with core-shell structure exhibits much higher catalytic activity for the direct oxidation of $NaBH_4$ than pure Au/C catalyst. A direct borohydride-hydrogen peroxide fuel cell, in which the Au-Pd/C with core-shell structure is used as the anode catalyst and the Au/C as the cathode catalyst, shows as high as 68.215 mW cm^{-2} power density.

1. Introduction

Fuel cells constitute an attractive class of renewable and sustainable energy sources alternative to conventional energy sources such as petroleum that has finite reserves. Among all types of fuel cells, the direct borohydride-hydrogen peroxide fuel cell (DBHFC) has recently attracted increasing attentions because of some excellent features such as high open circuit potential, low operation temperature, and high power density [1–8]. The DBHFC is comprised of BH_4^- oxidation at the anode and H_2O_2 reduction at the cathode; thus, it can be used as a promising power source for space and underwater applications. Generally, the key of development of DBHFC is anode electrocatalyst Cao et al. [9] have prepared Au/Ni-foam electrode by spontaneous deposition of Au nanoparticles on nickel foam substrates and achieved an open-circuit voltage of about 1.07 V and a peak power density of 100 mW cm^{-2} at 170 mA cm^{-2} and 0.6 V at 60°C. Chatenet et al. [10] reported that electrooxidation of BH_4^- can exchange about 7.5 electrons on Au and Ag electrodes in contrast to about 4 electrons on Pt electrode. The high electron utilization efficiencies of Au and Ag towards BH_4^- electrooxidation are attributed to their low activity towards BH_4^- hydrolysis. However, the catalyst, which causes the low activity towards BH_4^- hydrolysis, simultaneously has a low catalytic activity towards BH_4^- electrochemical oxidation reaction. Thus, it is very important for DBHFC application to develop high-activity electrocatalysts for the borohydride oxidation reaction (BOR).

In our previous works, high-activity catalysts such as carbon-supported hollow gold nanoparticles (HAu/C) [11, 12] and AuCo/C [13] have been studied. Usually, the core-shell structure is an effective morphology to enhance catalytic activity. The improvement of catalytic activity of core-shell bimetallic nanoparticles is attributed to the unique structure in electrocatalysis, which has gained much attention in recent years [14]. Besides, the activity of core-shell structure is related with the underlying interface between the core and shell metals due to the bimetallic mechanism [15]. It is reported that the core-shell nanoparticle catalysts such as Ni@Pd/MWCNTs [16] and Pt_{shell}-Au_{core}/C [17] have effectively enhanced the catalytic activity for the electrooxidation of methanol. Palladium is an appropriate choice as the shell of the catalyst since it has the similar catalytic activity as platinum, which is more expensive than the former. In this paper, carbon-supported bimetallic Au-Pd catalyst

with the core-shell structure was prepared by successive reduction method. The electrochemical performances for the borohydride oxidation reaction were examined by linear voltammetry, chronoamperometry, chronopotentiometry, and fuel-cell performance measurement.

2. Experimental

2.1. Preparation of Carbon-Supported Core-Shell Au-Pd Nanoparticles. The preparation of Au seed was reported elsewhere [18, 19]. Concisely, the citrate-stabilized Au nanoparticles were prepared by $NaBH_4$ reduction of 0.5 mM $HAuCl_4$ aqueous solution in the presence of trisodium citrate in 100 mL ice ultrapure (18.2 kΩ) water with vigorous stirring [20]. Stirring was continued for 12 h to decompose the unreacted $NaBH_4$. Then 0.25 mL 0.1 M H_2PdCl_4 aqueous solution and freshly prepared 1.25 mL 0.1 M ascorbic acid aqueous solution were added dropwise to the Au hydrosol. The solution was continuously stirred for 2 h and then added 50 mg Vulcan XC-72R carbon slurry (metal loading was 20 wt. %). After stirring 5 h, the suspension was filtrated to recover solid product, which was fully washed with water and alcohol. The recovered solid product was dried in vacuum at 80°C overnight. Comparatively, carbon-supported monometallic Pd and Au samples with the same overall metal loading were prepared by similar procedures.

2.2. Characterization of Anode Catalysts. The samples for transmission electron microscopy (TEM) were prepared by putting one drop of the sample slurry on a copper grid followed by drying in a desiccator. Electron micrographs were taken with a FEI Tecnai G2 microscope at 200 kV. A diffractometer (D/MAX-3C) was employed using Cu Kα radiation (λ = 1.54056 Å) and a graphite monochromator at 50 kV, 100 mA, to obtain XRD spectra of the samples. Continuous X-ray scans were carried out from 10° to 90° of 2θ. The UV-Vis spectra of the hydrosols were measured by a Lambda 25 spectrometer equipped with quartz cells.

2.3. Electrochemical Performance of Anode Catalysts. A conventional three-electrode cell was used to perform the electrochemical tests of the anode catalysts at 25°C with a CHI660A Electrochemistry Workstation. The Au-Pd/C was used as working electrode, an Ni foam mesh with 3×5 cm^2 as counter electrode and an Ag/AgCl, KCl_{std} as the reference electrode. The electrolyte was 0.1 M $NaBH_4$ + 3.0 M NaOH. The working electrode was prepared as follows: 5 mg of Au-Pd/C powder was dispersed by ultrasonic for 2 h in 0.5 mL blend solution of 0.125 mL 5 wt. % Nafion solution and 0.375 mL deionized water. Then 5 μL of slurry was pasted on the surface of the glassy carbon (GC) electrode (3 mm in diameter) which was polished to mirror by 0.5 μm alumina and sonicated 5 min prior to use. The dispersed catalyst on the GC surface was dried for 5 h at ambient temperature.

2.4. Fuel Cell Test. The performance of the direct $NaBH_4$-H_2O_2 fuel cell (DBHFC) was evaluated by a battery testing system at 25°C in standard atmospheric pressure. The schematic of direct $NaBH_4$-H_2O_2 fuel cell was shown in Figure 1, and it consisted of Au/C cathode, core-shell Au-Pd/C anode, activated Nafion 117 membrane separator, anolyte composed of 1 M $NaBH_4$ + 3 M NaOH, and catholyte composed of 2 M H_2O_2 + 0.5 M H_2SO_4. The fresh anolyte and catholyte were continuously supplied and withdrawn from the cell at a rate of 0.7 mL min^{-1} during the testing process. The load was applied in steps of 5 mA within the range of 0–150 mA. Each step lasted 2 min, and the current was continuously applied from one value to the next without disconnecting the cell.

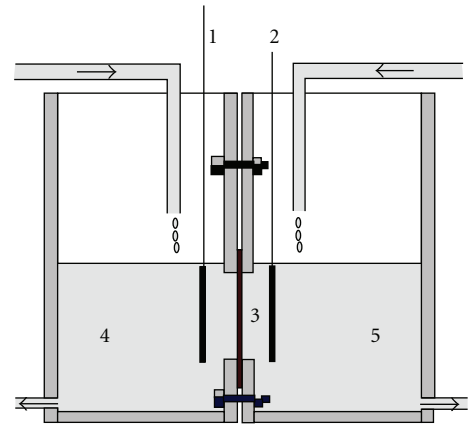

Figure 1: Simple schematic illustration of DBHFC (1) anode catalyst, (2) cathode catalyst, (3) the activated Nafion 117 membrane, (4) 1 M $NaBH_4$ + 3 M NaOH, and (5) 2 M H_2O_2 + 0.5 M H_2SO_4.

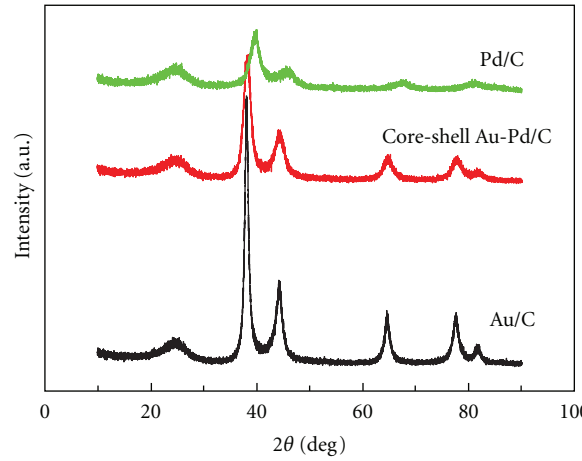

Figure 2: XRD patterns of Au/C, core-shell Au-Pd/C, and Pd/C.

The catalyst ink was made by mixing isopropyl Nafion solution and carbon-supported catalyst and coated onto stainless steel gauze. Then it was dried in vacuum at 80°C for 12 h and pressed at 16 MPa for 1 min. Finally, the loading mass of catalysts was about 4.5 mg cm^{-2}.

3. Results and Discussion

3.1. Physical Characterization. Figure 2 showed the XRD patterns of Au/C, core-shell Au-Pd/C, and Pd/C. As shown in Figure 2, the rather wide diffraction peaks at $2\theta \approx 25°$ in

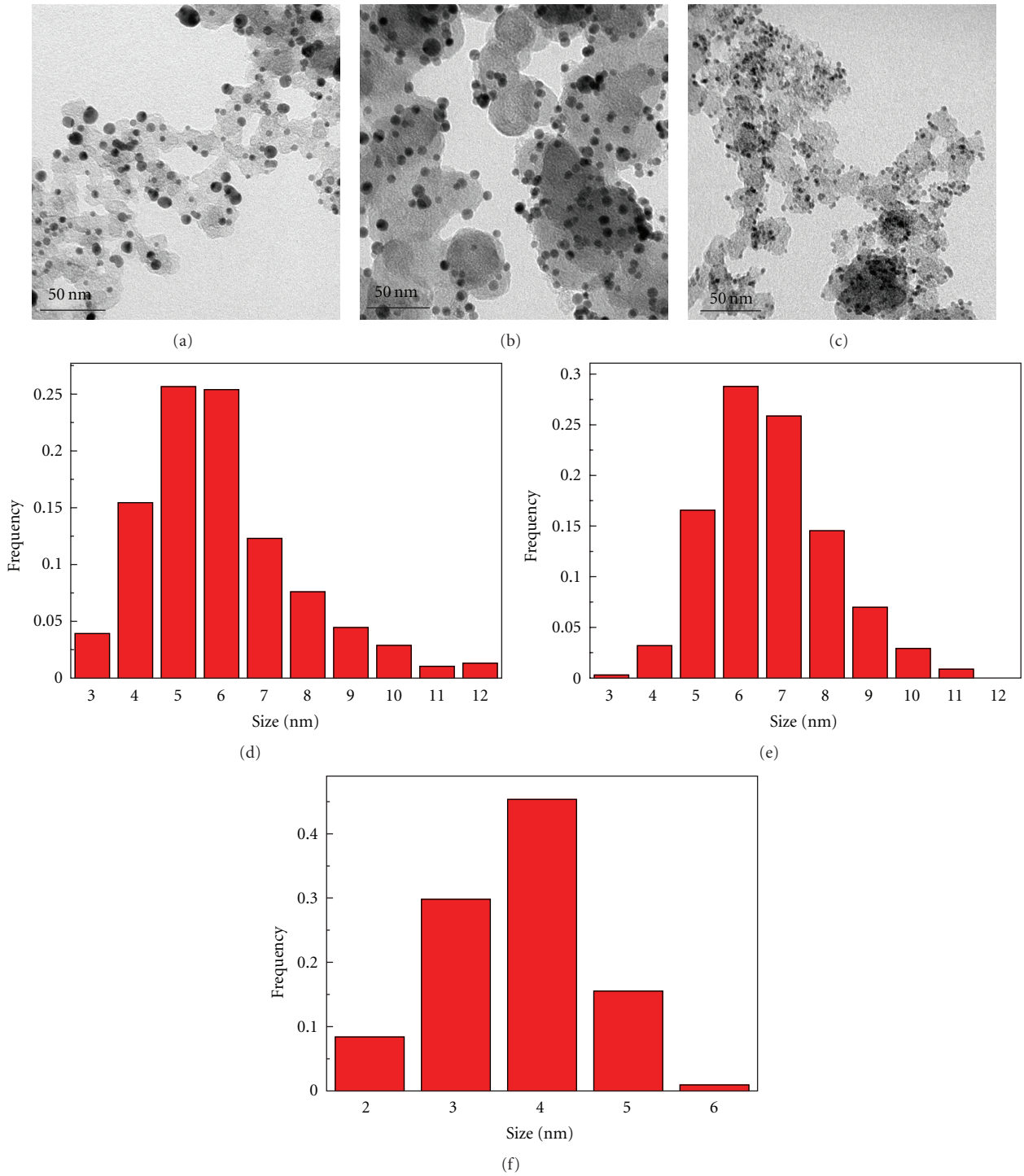

Figure 3: TEM images of Au/C (a), core-shell Au-Pd/C (b), and Pd/C (c) and their corresponding histograms on size distribution.

all three samples are attributed to Vulcan XC-72R carbon (002) crystal face. In Au and core-shell Au-Pd catalysts, there are other five main characteristic peaks, which could be attributed to the face-centered cubic (fcc) structure of crystalline Au (111), (200), (220), (311), and (222). These indicated the absence of both isolated large-size Pd particles and the bulk Au-Pd alloy phases in the core-shell Au-Pd/C catalyst. The morphologies and particle distributions of the carbon-supported Au/C, core-shell Au-Pd/C, and Pd/C samples were showed in Figure 3. The corresponding histograms on size distribution of electrocatalysts were also simultaneously given in Figures 3(d), 3(e), and 3(f). It could be seen from Figure 3 that the spheroidal nanoparticles were homogeneously dispersed on the surface of the carbon supporter. The average diameter of Au, core-shell Au-Pd, and Pd particles in samples from counting more than 300

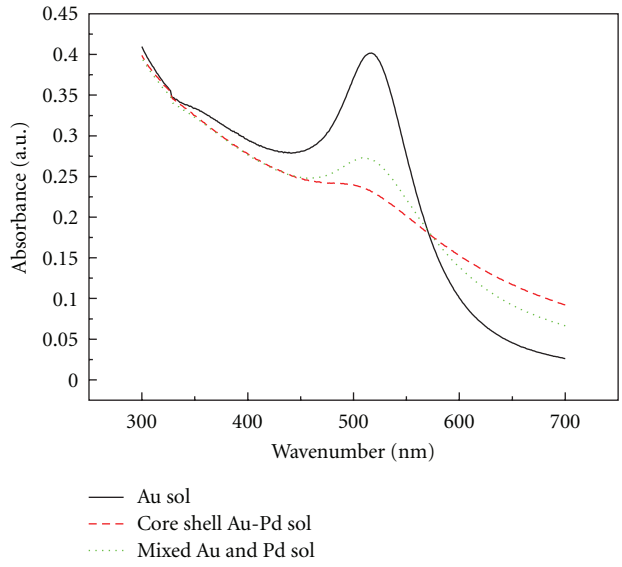

Figure 4: Absorption spectra of Au, core-shell Au-Pd, and mixed Au-Pd hydrosols before deposition on carbon.

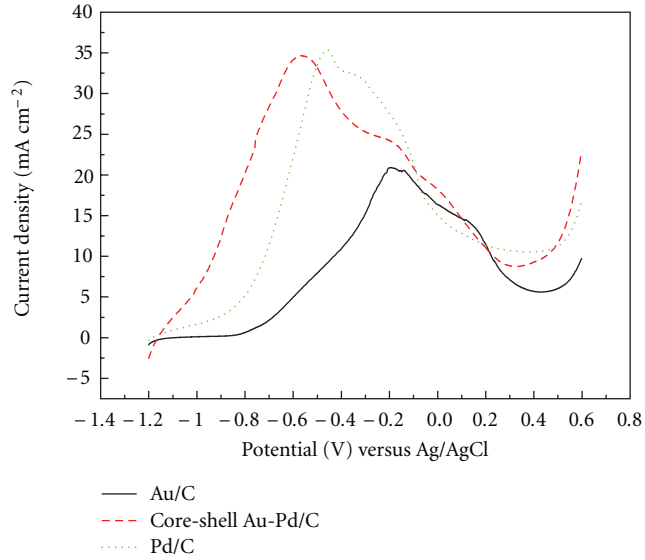

Figure 5: Linear sweep voltammogram of Au/C, core-shell Au-Pd/C, and Pd/C electrodes.

particles were about 5.955 nm, 6.705 nm, and 3.613 nm, respectively. Usually, the size of the particle with core-shell structure, D, can be calculated by [21]

$$D = D_{\text{core}}\left(1 + \frac{V_{\text{Pd}}[\text{Pd}]}{V_{\text{Au}}[\text{Au}]}\right)^{1/3}. \quad (1)$$

Here, D_{core} was the measured Au particles size; V_{Pd} and V_{Au} were the academic Pd and Au mole volume, respectively; [Pd] and [Au] were the overall concentrations of the two metals involved, respectively. It had been found from the above formula that the calculated size of core-shell Au-Pd particle was 6.719 nm, which is close to actually measured particle size (6.705 nm). Besides, the calculated Pd shell thickness was about 0.375 nm.

The absorption spectra of Au hydrosol, core-shell Au-Pd hydrosol, and mixed Au-Pd hydrosol were shown on Figure 4. The absorption peak positioned at 516 nm, which was ascribed to the surface plasmon resonance (SPR) of Au, could be clearly observed for Au hydrosol. For the mixed Au-Pd hydrosol, the Au plasmon absorption peak declined slightly because of the decrease of the Au hydrosol concentration. However, for the core-shell Au-Pd hydrosol, the remaining Au plasmon absorption peak indicated that the Pd shell was not too thick to overwhelm the SPR response of the Au nanoparticles [22].

3.2. Electrochemical Performance of Anode Catalysts. Figure 5 showed the linear sweep voltammogram (LSV) of different catalysts in 0.1 M $NaBH_4$ + 3.0 M NaOH solution at 25°C at a potential sweep rate of 20 mV s^{-1} in the potential range of −1.2 V to 0.6 V versus Ag/AgCl. The Au-Pd/C with core-shell structure and Pd/C exhibited more negative initial reaction potentials than Au/C due to the BH_4^- hydrolysis. The current densities of Au/C, core-shell Au-Pd/C, and Pd/C were 20.80 mA cm^{-2}, 24.35 mA cm^{-2}, and 27.89 mA cm^{-2} at −0.2 V versus Ag/AgCl, respectively. The peak current density of Au-Pd/C (34.65 mA cm^{-2}) was nearly close to Pd/C (35.44 mA cm^{-2}), which was about 1.7 times higher than that of Au/C (20.80 mA cm^{-2}). Besides, the area enclosed by LSV on core-shell Au-Pd/C electrode was apparently bigger than that on Au/C and Pd/C electrodes. Obviously, the above results indicated that the core-shell Au-Pd/C catalyst had much better catalytic activity than pure Au and Pd catalysts. Moreover, the core-shell Au-Pd/C (4.25 wt. % Pd loading) was more economical than Pd/C (20 wt. % Pd loading). The reasons why the core-shell Au-Pd/C enhanced the catalytic activity of the borohydride oxidation reaction could correlate with the long-range electromagnetic enhancement between the Au core and the Pd shell [23].

Chronopotentiometry was a usefully qualitative screening method for catalyst since it simulated the constant current operation of a fuel cell. Figure 6 showed the chronopotentiometry curves of BH_4^- oxidation on the Au/C, core-shell Au-Pd/C, and Pd/C at a current density of 8.5 mA cm^{-2} in a solution of 0.1 M $NaBH_4$ + 3 M NaOH, respectively. The open-circuit potentials (OCPs) were −0.953 V versus Ag/AgCl for Au/C, −1.203 V versus Ag/AgCl for core-shell Au-Pd/C, and −1.188 V versus Ag/AgCl for Pd/C. After 120 s, the operating potential for Au/C, core-shell Au-Pd/C, and Pd/C was −0.653 V, −0.920 V, and −0.800 V, respectively. Therefore, it can be expected that the core-shell Au-Pd/C catalyst had higher direct electrooxidation catalytic activity and power output than those of Au/C and Pd/C under the same experimental condition, which also suggested the possibility of potentially obtaining a higher power output.

In chronoamperometry experiments (Figure 7(a)), the potential was stepped from −1.2 to −0.2 V versus Ag/AgCl in 0.1 M $NaBH_4$ + 3 M NaOH solution. At the beginning of the experiment, the initial current densities of three carbon-supported catalysts corresponded mainly to double-layer charging. The core-shell Au-Pd/C and Pd/C showed

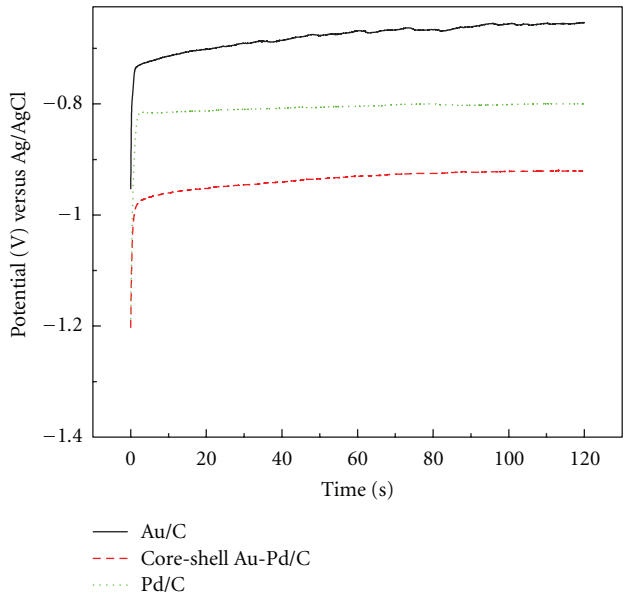

Figure 6: Chronopotentiometry curves of Au/C, core-shell Au-Pd/C and Pd/C electrodes.

a gradual current density decay with the increase of the time before a steady current density was reached. However, the current density slowly decayed on Au/C, which would be related to the formation of borohydride oxidation products [10]. The current in the steady-state region represented the current of the electrochemical reaction, so it could reflect partly the electrocatalytic activity of the electrodes. As being shown in Figure 7(a), the core-shell Au-Pd/C catalyst maintained a higher borohydride oxidation current density than those of the other two catalysts. In order to analyze well the electrocatalytic activity of BH_4^- on the different catalysts, the chronoamperometry results were summarized as a Cottrell plot in Figure 7(b). The approximate constancy of the $It^{1/2}$ versus t on Au/C in the steady process could be attributed to electrode deactivation. On the other hand, the increase of $It^{1/2}$ value with the increase of the time on core-shell Au-Pd/C and Pd/C indicated that neither the intra-catalyst layer diffusion nor the external mass transfer of BH_4^- became rate limiting under the employed conditions [24]. And core-shell Au-Pd/C had larger $It^{1/2}$ value than Pd/C, which indicates the higher activity of oxidation of BH_4^-. Moreover, the increasing value suggested the surfaces of Au-Pd/C and Pd/C are not poisoned during the experiment process.

3.3. Fuel Cell Performance. The cell polarization and power density curves for DBHFC using 1 M $NaBH_4$ + 3 M NaOH solution as fuel and 2 M H_2O_2 + 0.5 M H_2SO_4 solution as oxidant were presented in Figure 8. In the experimental cell, the Au/C was used as the cathode catalyst and Au/C, core-shell Au-Pd/C, and Pd/C as the anode catalyst, respectively. The cell voltage had an initially abrupt reduction at the range of 0–10 mA cm^{-2} current density on Au/C, which showed a kinetic process of electrochemistry polarization. For the Pd/C and core-shell Au-Pd/C electrodes, the cell

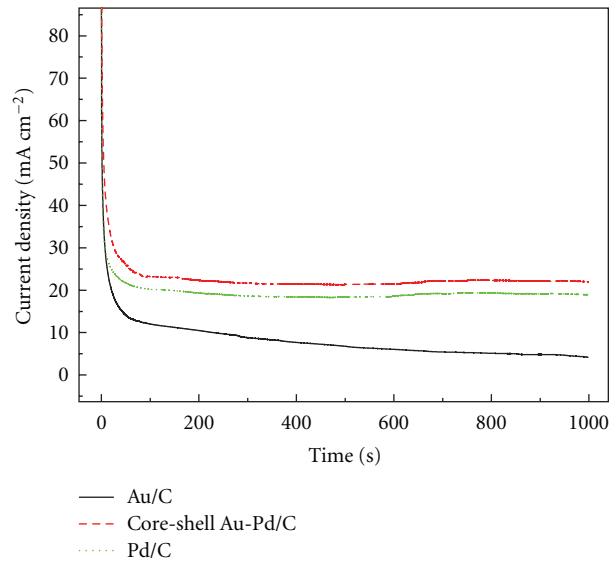

(a)

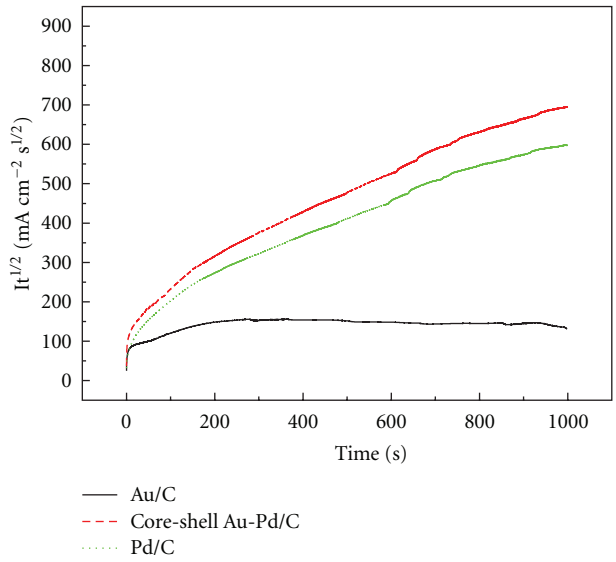

(b)

Figure 7: (a) Chronoamperometry curves of BH_4^- oxidation on different anode catalysts and (b) Cottrell's plot generated from the chronoamperometry data.

voltage curves linearly decreased with the increase of current density, indicating a strong dependence of cell performance on the ohmic resistance (mainly ohmic polarization). In addition, the slope of the polarization curve on the core-shell Au-Pd/C catalyst electrode was lower than that on Pd/C. This phenomenon showed that the core-shell Au-Pd/C catalyst can decrease oxidation overpotential of BH_4^- and improve the performance of DBHFC. Furthermore, the core-shell Au-Pd/C exhibited a maximum power density of 68.215 mW cm^{-2} at a current density of 90.1 mA cm^{-2} and a cell voltage of 0.757 V at 25°C.

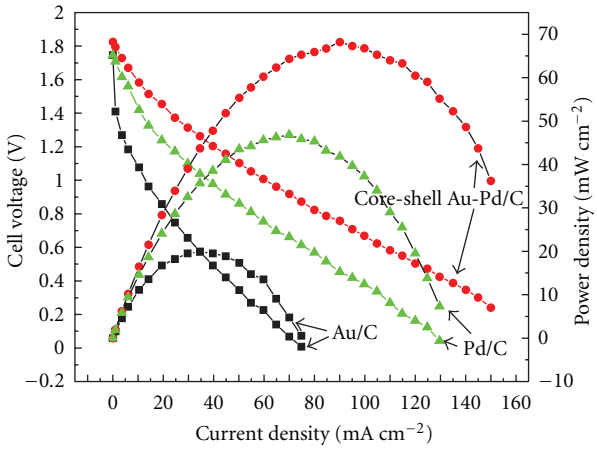

FIGURE 8: Cell polarization curves and power density curves of the DBHFC using various anode catalysts.

4. Conclusions

The carbon-supported bimetallic Au-Pd catalyst with the core-shell structure was successfully prepared by successive reduction method. The spheroidal Au-Pd nanoparticles were homogeneously dispersed on the surface of carbon supporter. Compared with carbon-supported monometallic Au and Pd catalysts, the core-shell Au-Pd catalyst had an enhanced electrocatalytic activity for the BH_4^- electrooxidation. The fuel cell using core-shell Au-Pd as anode catalyst presented a maximum power density of 68.215 mW cm^{-2} and a cell voltage of 0.757 V in 1 M $NaBH_4$ + 3 M NaOH solution at 25°C. Therefore, the carbon-supported bimetallic Au-Pd catalyst with the core-shell structure would be a promising anode electrocatalyst for the application of DBHFC.

Acknowledgments

This work was financially supported by the National Natural Science Foundation of China (Grants no. 20871101 and 51072173), the Doctoral Fund of Ministry of Education of China (Grant no. 20094301110005), and the project supported by Science and Technology Department of Hunan Province (Grant no. 2010GK3181).

References

[1] J. Ma, N. A. Choudhury, and Y. Sahai, "A comprehensive review of direct borohydride fuel cells," *Renewable and Sustainable Energy Reviews*, vol. 14, no. 1, pp. 183–199, 2010.

[2] S. Y. Park, D. W. Lee, I. S. Park, Y. K. Hong, Y. M. Park, and K. Y. Lee, "The effective bimetallic component of Pd-Au/C for electrochemical oxidation of borohydrides," *Current Applied Physics*, vol. 10, no. 2, pp. S40–S43, 2010.

[3] R. K. Raman, N. A. Choudhury, and A. K. Shukla, "A high output voltage direct borohydride fuel cell," *Electrochemical and Solid-State Letters*, vol. 7, no. 12, pp. A488–A491, 2004.

[4] P. He, Y. Wang, X. Wang et al., "Investigation of carbon supported Au-Ni bimetallic nanoparticles as electrocatalyst for direct borohydride fuel cell," *Journal of Power Sources*, vol. 196, no. 3, pp. 1042–1047, 2011.

[5] G. H. Miley, N. Luo, J. Mather et al., "Direct $NaBH_4/H_2O_2$ fuel cells," *Journal of Power Sources*, vol. 165, no. 2, pp. 509–516, 2007.

[6] C. P. de León, F. C. Walsh, A. Rose, J. B. Lakeman, D. J. Browning, and R. W. Reeve, "A direct borohydride-Acid peroxide fuel cell," *Journal of Power Sources*, vol. 164, no. 2, pp. 441–448, 2007.

[7] L. Gu, N. Luo, and G. H. Miley, "Cathode electrocatalyst selection and deposition for a direct borohydride/hydrogen peroxide fuel cell," *Journal of Power Sources*, vol. 173, no. 1, pp. 77–85, 2007.

[8] W. Haijun, W. Cheng, L. Zhixiang, and M. Zongqiang, "Influence of operation conditions on direct $NaBH_4/H_2O_2$ fuel cell performance," *International Journal of Hydrogen Energy*, vol. 35, no. 7, pp. 2648–2651, 2010.

[9] D. Cao, Y. Gao, G. Wang, R. Miao, and Y. Liu, "A direct $NaBH_4$-H_2O_2 fuel cell using Ni foam supported Au nanoparticles as electrodes," *International Journal of Hydrogen Energy*, vol. 35, no. 2, pp. 807–813, 2010.

[10] M. Chatenet, F. Micoud, I. Roche, and E. Chainet, "Kinetics of sodium borohydride direct oxidation and oxygen reduction in sodium hydroxide electrolyte. Part I. BH_4^- electro-oxidation on Au and Ag catalysts," *Electrochimica Acta*, vol. 51, no. 25, pp. 5459–5467, 2006.

[11] J. Wei, X. Wang, Y. Wang, Q. Chen, F. Pei, and Y. Wang, "Investigation of carbon-supported Au hollow nanospheres as electrocatalyst for electrooxidation of sodium borohydride," *International Journal of Hydrogen Energy*, vol. 34, no. 8, pp. 3360–3366, 2009.

[12] J. Wei, X. Wang, Y. Wang et al., "Carbon-supported au hollow nanospheres as anode catalysts for direct borohydride-hydrogen peroxide fuel cells," *Energy and Fuels*, vol. 23, no. 8, pp. 4037–4041, 2009.

[13] F. Pei, Y. Wang, X. Wang et al., "Performance of supported Au-Co alloy as the anode catalyst of direct borohydride-hydrogen peroxide fuel cell," *International Journal of Hydrogen Energy*, vol. 35, no. 15, pp. 8136–8142, 2010.

[14] R. W. J. Scott, O. M. Wilson, S. K. Oh, E. A. Kenik, and R. M. Crooks, "Bimetallic palladium—Gold dendrimer-encapsulated catalysts," *Journal of the American Chemical Society*, vol. 126, no. 47, pp. 15583–15591, 2004.

[15] D. R. Rolison, "Catalytic nanoarchitectures—the importance of nothing and the unimportance of periodicity," *Science*, vol. 299, no. 5613, pp. 1698–1701, 2003.

[16] Y. Zhao, X. Yang, J. Tian, F. Wang, and L. Zhan, "Methanol electro-oxidation on Ni@Pd core-shell nanoparticles supported on multi-walled carbon nanotubes in alkaline media," *International Journal of Hydrogen Energy*, vol. 35, no. 8, pp. 3249–3257, 2010.

[17] N. Kristian and X. Wang, "Pt_{shell}-Au_{core}/C electrocatalyst with a controlled shell thickness and improved Pt utilization for fuel cell reactions," *Electrochemistry Communications*, vol. 10, no. 1, pp. 12–15, 2008.

[18] K. C. Grabar, K. J. Allison, B. E. Baker et al., "Two-dimensional arrays of colloidal gold particles: a flexible approach to macroscopic metal surfaces," *Langmuir*, vol. 12, no. 10, pp. 2353–2361, 1996.

[19] N. R. Jana, L. Gearheart, and C. J. Murphy, "Wet chemical synthesis of high aspect ratio cylindrical gold nanorods," *Journal of Physical Chemistry B*, vol. 105, no. 19, pp. 4065–4067, 2001.

[20] A. Gole and C. J. Murphy, "Seed-mediated synthesis of gold nanorods: role of the size and nature of the seed," *Chemistry of Materials*, vol. 16, no. 19, pp. 3633–3640, 2004.

[21] A. Henglein, "Preparation and optical aborption spectra of $Au_{core}Pt_{shell}$ and $Pt_{core}Au_{shell}$ colloidal nanoparticles in aqueous solution," *Journal of Physical Chemistry B*, vol. 104, no. 10, pp. 2201–2203, 2000.

[22] W. Zhou and J. Y. Lee, "Highly active core-shell Au@Pd catalyst for formic acid electrooxidation," *Electrochemistry Communications*, vol. 9, no. 7, pp. 1725–1729, 2007.

[23] J. W. Hu, Y. Zhang, J. F. Li et al., "Synthesis of Au@Pd core-shell nanoparticles with controllable size and their application in surface-enhanced Raman spectroscopy," *Chemical Physics Letters*, vol. 408, no. 4–6, pp. 354–359, 2005.

[24] M. H. Atwan, C. L. B. Macdonald, D. O. Northwood, and E. L. Gyenge, "Colloidal Au and Au-alloy catalysts for direct borohydride fuel cells: electrocatalysis and fuel cell performance," *Journal of Power Sources*, vol. 158, no. 1, pp. 36–44, 2006.